Designing Peptoid-based Cofactor-free Catalysts for Enhanced CO_2 Hydration

Ling Dai

A thesis
submitted in partial fulfillment of the
requirements for the degree of

Master of Science

University of Washington
2025

Reading Committee:
Chun-Long Chen
Robert E. Synovec

Program Authorized to Offer Degree:
Chemistry

Abstract

Designing Peptoid-based Cofactor-free Catalysts for Enhanced CO_2 Hydration

Ling Dai

Chair of the Supervisory Committee:
Chun-Long Chen
Department of Chemistry

Efficient carbon dioxide hydration is a key step in carbon capture and utilization technologies. Natural carbonic anhydrase catalyzes this reaction with excellent efficiency yet suffers from low abundance and poor stability for industrial usage. Peptoid-based enzyme mimetics have been offered as a promising solution. Referring to the structural similarities between peptoids and peptides, a series of peptoid-based biomimetic catalysts have been designed and synthesized. In this thesis, we have performed systematic evaluations of peptoid-based catalysts as CA mimetics. By investigating the influence of morphology of peptoid-based nanostructures on catalytic activity, we first verified that the catalytic activity of mimetics is brought by a similar structure to the active site of CA. Then results showed that crystalline nanosheet with higher solvent- accessible surface areas exhibited higher catalytic activity. Also, by investigating the influence of ligand-metal coordination, we identified structural features that promote or hinder catalytic activity. Furthermore, stability tests conducted on a cofactor-free catalyst, Nbrpe6cyclenHis3, which further confirmed the high structural and activity stability of peptoid-based catalyst.

I. Section 1. Introduction to Peptoid and application

1.1 Peptoid, Supramolecular Chemistry, and Self-assembly

Peptoids, or poly-N-substituted glycines, are synthetic polymers structurally similar to peptides but with improved stability, chemical diversity, and synthetic control. Unlike peptides, peptoids have side chains attached to the nitrogen atom of the backbone rather than to the α-carbon[1]. Such structure eliminates backbone hydrogen bond donors and therefore enhances their resistance to proteolytic degradation. These features make peptoids a versatile platform for designing sequence-defined molecules with programmable structure and function, suitable for applications in nanomaterials[1-4].

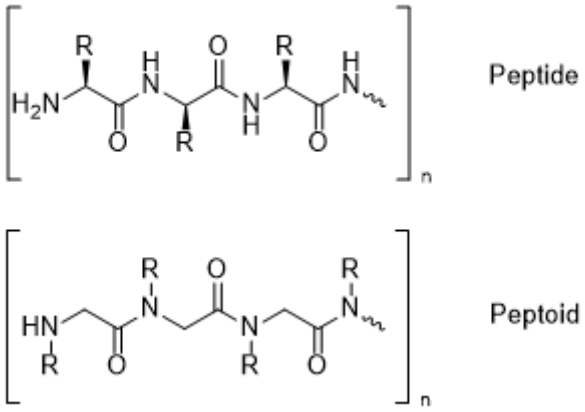

Fig 1.1 Schemes of a general peptide and peptoid sequence

Supramolecular chemistry studies how molecules interact through non-covalent forces, such as hydrogen bonding, hydrophobic effects, van der Waals forces, π–π interactions[5-7], and metal coordination, to form well-defined nanostructures. It is an enchanting field that is located at the border among physics, chemistry and biology. A fundamental goal of this field is to understand how these relatively weak interactions collectively create ordered, stable and functional molecular structures[8]. Like peptide, peptoids have high flexibility on their

sequence-specific side chains, they can be tuned to optimize these noncovalent interactions[3]. Such design flexibility allows peptoid to form ordered structures[1, 2]. For instance, lipid-like peptoids with designed hydrophobic and hydrophilic domains can self-assembled into crystalline nanotubes or nanosheets controlled by the hydrophobic interactions among non-polar side chains[2, 9, 10]. In 2007, a successful example of a self-assembled peptide-based nanofiber catalyst that emulate enzyme was designed and synthesized[5]. Peptide amphiphiles (PAs) assembled into nanofibers by hydrophobic collapse of the alkyl tails and β-sheet formation among the peptidic segments. It has also shown the ability to catalyze ester hydrolysis[5]. By incorporating specific functional groups or coordination sites into the side chains or as the ligands, supramolecular assemblies from sequence-defined molecules can be developed to mimic the biological structures of natural enzymes for catalytic reactions[11, 12]. Hydrogen-bonded coordination frameworks have shown the capability to incorporate guest molecules due to structural flexibility imparted by non-covalent interactions, suggesting potential for use as responsive catalytic systems[13]. Specifically, introducing flexible linkers or functional groups near metal centers allows such frameworks to undergo reversible structural transformations upon guest molecule exchange or ligand rearrangement, thereby stabilizing intermediates critical for catalytic activity. Inspired by the successful development of peptide-based catalysts, research on the synthesis and application of biomimetic catalysts has also gained increasing attention. However, CA mimics formed through peptide assembly often having difficult to adjust the local environment around active sites without compromising the integrity of the assembled nanostructures[14,15]. Benefiting from their simpler and more stable chemical structures, as well as higher flexibility in designing side-chain groups, peptoids are

emerging as promising candidates for catalytic materials. In this thesis, a peptoid sequence, Nbrpe6cyclenHis3 that was originally designed to mimic carbonic anhydrase could self-assemble to crystalline nanosheet meanwhile having the similar structure to that of the carbonic anhydrase's active site. A review by Liu et al in 2022 discusses the design of peptide-based artificial enzymes that utilize coordination-driven self-assembly to achieve enzyme-like catalytic activities[6]. The authors highlighted how metal ions can induce the self-assembly of peptide-based structures, leading to the formation of active sites that resemble those of natural enzymes. This mechanism not only replicates the structural aspects of enzymes but also provides functional catalytic properties.

Trinh et al. demonstrated such coordination-driven assembly by introducing metal-binding ligands into peptoid sequences to form membranes mimicking the catalytic sites of Pseudomonas diminuta phosphotriesterase (PTE)[7]. These membranes exhibited strong catalytic activity, proving the effectiveness of supramolecular strategies in creating functional biomimetic materials.

Self-assembly refers to the process of spontaneous organization of individual monomers into ordered structures or patterns without external direction. Typically, when the ordered state forms as a system approaches equilibrium, reducing its free energy, it is defined as static self-assembly. Inspired by the commonly found examples of self-assembly in biological systems such as protein folding, combined with the increasing need of nano biomimetic materials, self-assembled peptoid has been studied and developed as biomimetic materials. Peptoid

biomimetics could combine the advantages of both synthetic polymers and biomolecules, since it has highly programmable backbone. Peptoid is a promising platform to build biomimetic materials. Olivier et al reported an antibody mimetic constructed from peptoid nanosheet[8]. They used the automated solid phase sub-monomer synthesis method to obtain a library of individual loopoid strands. These loopoid strands were then used for supramolecular assembly. Then the Förster resonance energy transfer is used to test the binding affinity of the assembled loopoid strands with target proteins. The results showed that peptoid sequences have high binding specificity with anthrax protective antigen. Moreover, due to the chemical properties of the peptoid, these nanosheets were resistant to proteolytic degradation. Their results proved that biomimetic materials made by peptoid could be not only specific but also stable. Jian et al. reported a series of peptoid/hemin enzymatic mimetics with natural peroxidase-like activities[10]. These enzymatic mimetics exhibited high performance in lignin depolymerization, which is crucial in many industrial processes. The peptoids used to build the en1zymatic mimetics mainly consist of two parts: the structure-defining domain, which includes several hydrophilic and hydrophobic groups responsible for forming nanotubes, and the terminal binding domain with coordination sites such as [2-(4-imidazolyl)ethylamine]glycine, [2-(4-pyridyl)ethylamine]glycine, or N-[2-(1H-indol-3-yl)ethyl]glycine that can bind with hemin to mimic the active site of natural peroxidase. These peptoid/hemin enzymatic mimetics had decent catalytic activities and were more stable and easier to produce compared to natural peroxidase. Trinh et al developed a series of metal-containing peptoid membranes that mimic natural enzyme pseudomonas diminuta phosphotriesterase (PTE) in 2023. PTE is the most efficient enzyme for toxic

organophosphates degradation[7]. However, it is difficult to extract or produce for larger scale use. Moreover, as a natural enzyme, PTE enzymes could be easily denatured, which makes it costly to store. To solve this problem, Trinh et al. introduced small-molecule metal-binding ligands that mimic the active site of PTE into sequence-defined peptoids and used these peptoids to build membranes by self-assembly. These peptoid membranes were proved to have high catalytic activity for OP degradation and they were resistant to extreme pH, temperature and not easy to dissolve in organic solvents. Such properties make it a promising substitution for PTE.

1.2 Application: Biomimetics to catalyze Carbon Dioxide Hydration

Efficient carbon dioxide (CO_2) capture and conversion are critical for addressing global climate change and advancing carbon-neutral technologies, such as direct air capture and CO_2 to fuel conversion[11]. However, the hydration of CO_2 into bicarbonate ions (HCO_3^-) is naturally slow, with approximate reaction rate constant (k_1) of 0.037 s^{-1}. Such a slow rate limits overall efficiency and increasing operational costs in the capture and conversion processes. Due to its slow kinetics, enzymes like carbonic anhydrase (CA), a natural carbon dioxide hydratase, has attracted much attention for its potential applications[11]. It catalyzes hydration through a mechanism centered on a Zn^{2+} ion at its active site[12,13,17]. During this process, the Zn^{2+} ion is coordinated by three histidine residues and a water molecule or OH^- ion. The Zn bound hydroxide ion acting as a nucleophile, attacks the electrophilic carbon of CO_2 to form HCO_3^-. A nearby proton shuttle facilitates the removal of the proton generated during the reaction. This proton is transferred to the surrounding solvent and regenerating the

hydroxides that allows enzyme to continue its catalytic cycle[17]. CA exhibits excellent catalytic activity in CO_2 hydration that accelerates this reaction approximately 10^6 to 10^7-fold[12,13,16].

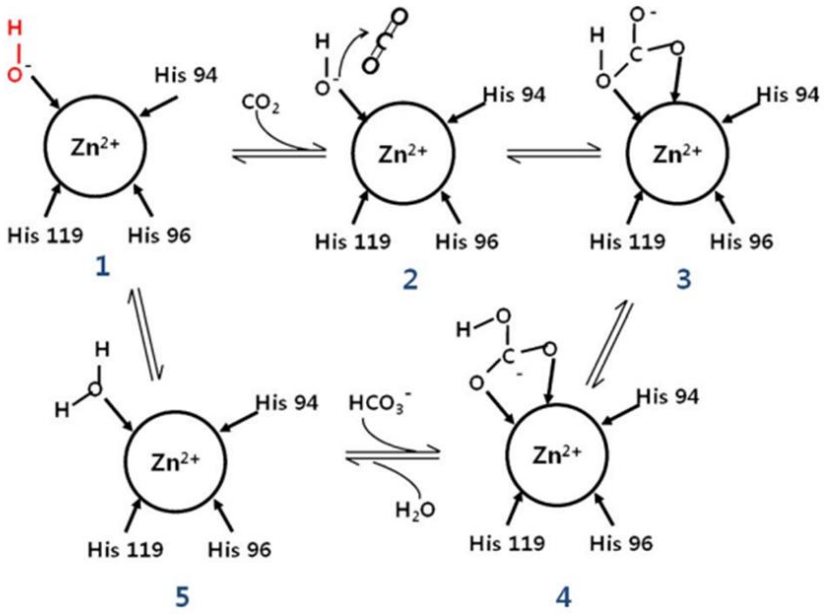

Fig1.2 Mechanism of CA catalyzes CO_2 hydration

However, similar to the use of PTE, the practical application of natural CA faces several challenges. One of the major limitations is the difficulty of obtaining CA in large quantities through natural extraction. Since CA is typically found in organisms with low abundance[17]. Although recombinant expression systems have been developed to produce CA, these methods remain costly and require specialized conditions to maintain enzyme activity[16]. CA, as a natural enzyme, exhibited relatively poor long-term stability, particularly under industrial conditions such as high temperature. CA tends to denature at temperatures above 60 ℃ and loses its activity under extreme pH conditions. It would also become unstable in the presence of organic solvents[17]. Suggested by Silverman et al., one of the main reasons of CA losing its catalytic activity is that natural enzymes like CA typically rely on metal ions or other complex organic cofactors to perform catalytic functions[18]. However, under harsh conditions,

typically away from physiological pH, these cofactors could easily be degraded or dissociated, leading to a loss of enzyme activity[19,20]. These factors made CA unsuitable for continuous or mass-scale use. To address these limitations, recent efforts have focused on developing enzyme biomimetics with improved stability or function without the need for metal ion cofactors. These cofactor-free structures offer a promising alternative, combining functional catalytic behavior with enhanced durability and environmental compatibility. Liu et al. has synthesized cofactor-free poly-peptide material that can effectively mimic the natural oxidase's enzymatic activity[21]. A 15-mer polyhistidine peptide could self-assembled into crystalline nanosheets with peroxidase-like catalytic activity. The catalytic mechanism involves the periodic alignment of imidazole groups, which act as electron donors and proton shuttles, stabilizing reaction intermediates during the oxidation of substrates like H_2O_2. These histidine-containing assemblies exhibited robust environmental tolerance, maintaining full structural integrity and enzymatic function after 10 cycles of heating at 75 ℃ and cooling at 25℃, as well as acidification at pH 1.0[21].

In this study, inspired by the structural similarity between peptoids and peptides, series of sequence-defined peptoids that mimic the active site of CA were designed and synthesized. By incorporating specific ligands into the peptoid backbone, the morphology and microenvironment of the binding site can be tuned. To systematically evaluate all sequences' catalytic activities, we have chosen some representative sequences to establish comparison groups. The first group compared the catalytic activity of unassembled peptoid monomers versus its self-assembled crystalline nanosheets, aiming to compare the effect of crystallinity

to the activity. Previous study has shown that supramolecular nanostructures can regulate catalytic efficiency[22]. Our data later confirmed that the catalytic activity is the result of the properly folded nanostructures rather than the monomers or ions which might reduce the activation energy non-specifically. The second group compared crystalline nanosheets and amorphous nanostructures assembled from similar sequences that both containing three imidazole ligands, examining how structural morphology influences catalytic function. The third group focused on active site's microenvironmental effects, comparing sequences that are incapable of forming a ternary complex with one that could. Interestingly, the data showed that some sequences' catalytic activities decreased with the coordination of metal ion. Such phenomenon is contradicted to our initial expectation. Later we suppose that it may due to the steric hindrances that limit the proper self-assemble or the coordination of the sequences. Based on this fact and combined with the example from previous study showcased a peptide-based catalyst that does not require cofactors to achieve enzymatic function[21]. We compared the catalytic performance of a specific peptoid sequence assembled in the presence of Zn^{2+} ions with that assembled without them, to evaluate whether coordination with metal ions enhances or is necessary for catalytic activity. All sequences' catalytic activities were characterized by using a p-nitrophenol (p-NP) assay under room temperature unless otherwise specified. Notably, the histidine-containing sequence exhibited the highest catalytic efficiency, comparing to natural CA in some conditions.

Furthermore, stability tests were performed under various conditions for the histidine-containing sequence, these self-assembled peptoid structures maintained their structural

integrity after a 2-hour incubation in different solvents at 90℃, exhibiting their excellent thermal and chemical stability. This level of robustness is a significant advantage over many other catalytic systems, including natural CA, which is known to denature at temperatures above 60 °C and lose activity under harsh chemical environments. The enhanced robustness of peptoid-based catalysts not only enables their use in industrial conditions but also improves the reusability.

1.3 Cofactor Free System

Another major factor causing CA to lose its catalytic activity is the dissociation of cofactors in a harsh environment. To further improve the stability of peptoid-based catalysts, a cofactor-free system was proposed. Liu et al has synthesized and evaluated the activity of cofactor-free peptide biomimetics[19]. According to their findings, histidine residues with specific length would self-assemble to highly crystalline nanosheet through hydrogen bonding and π–π stacking and cofactor-free enzyme mimics obtained have also been reported to have high catalytic activity. This may be due to the formation of imidazolyl-rich sites after self-assembly, leading to base mediated ester hydrolysis. Combined with the nature that peptide shares similar structure with peptoid, histidine containing sequences were synthesized. According to our group's previous study, these sequences showed high catalytic activity. To optimize the performance of His-Zn^{2+} coordination, peptoid with varied number of histidine were compared. The sequence with 3 histidine groups exhibited significantly higher activity than that of others. The sequence with 3 N-histidine shows the highest k/k_{uncat} ratio which is 59.7. A decrease in activity observed in the sequence with 4 N-histidine,

showing a k/k_{uncat} = 50.2 and the sequence with 2 N-histidine's catalytic activity is almost halved. To achieve cofactor-free catalysis and further enhance the catalytic activity, a cyclen group was added to the sequence. Nbrpe6cyclenHis3, showed excellent catalytic activity without any cofactor. Inspired by natural oxidases and recent findings on self-assembled histidine-rich peptides, such as findings described by Liu et al.[19], cofactor-free catalysis can happen from cooperative interactions among neighboring histidine residues arranged through supramolecular assembly. These assemblies enable efficient catalysis of redox and hydrolysis reactions by forming dense imidazole-rich environments that mimic active sites in metalloenzymes like carbonic anhydrase or peroxidases. Similarly, in our peptoid-based system, cyclen acts as a rigid scaffold that not only enhances the local density and orientation of histidine residues but also facilitates their cooperative function through hydrogen bonding and π–π stacking. This structured environment supports substrate binding and activation, similar to the role of coordinated Zn^{2+} in natural enzymes. Thus, cyclen plays a crucial role in synthesizing peptoid catalyst that exhibit robust, reusable, and cofactor-free catalytic activity under conditions that typically deactivate natural enzymes.

1.4 Peptoid Synthesis

Peptoids, unlike peptides, feature a glycine backbone with side chains attached to the nitrogen atom rather than the α carbon. Although this modification introduces only a minor change in chirality, it significantly reduces structural complexity. By replacing the hydrogen on the nitrogen with a side chain, peptoids eliminate the potential for intermolecular hydrogen bonding. This streamlined backbone design allows more straightforward synthesis and programming, making peptoids highly versatile for various applications[9]. By varying side chains and ligands, we were able to precisely construct the morphology of the nanomaterial and therefore systematically compare their properties. Such tunability shows the potential of peptoids as a promising tool in biomimetic catalysts and other functional material applications. Generally, peptoid can be synthesized using solid phase submonomer synthesis. The reaction starts with an acylation of a resin-bound amine. Then the ligands or the side chain groups will be added for the displacement or nucleophilic substitution. Once the desired sequence is formed, the last monomer will be cut off from the resin. This method can be carried out through an automated synthesizer.

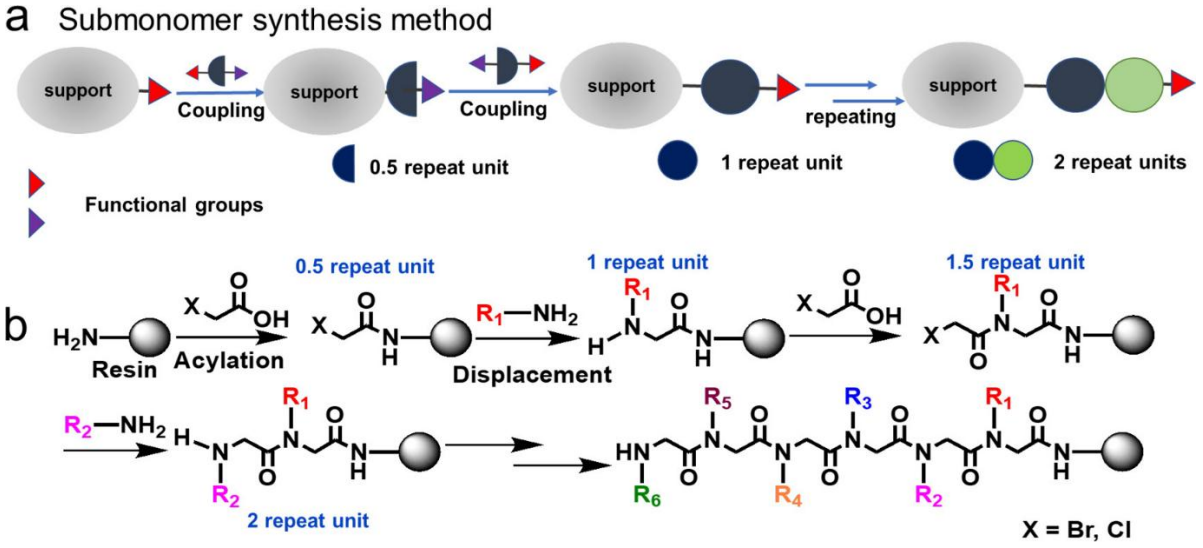

Fig1.3 a) Submonomer synthesis illustration[4] b) General schemes of peptoid synthesis[4]

1.5 Hydrolysis Activity Assay

The Nitrophenol Acetate (NPA) assay is a widely used colorimetric assay to determine the esterase activity of enzymes, including carbonic anhydrase[23]. Besides catalytic activity for CO_2 hydration, CA also has catalytic hydrolysis activity of esters. Natural carbonic anhydrase contains a Zn^{2+} ion at its active site. Zn^{2+} ion polarizes the bound H_2O molecule and a nearby histidine acts as a proton shuttle to facilitate the removal of a proton from the H_2O molecule, forming a Zn^{2+}-OH^- complex. This hydroxide complex acts as a strong nucleophile to attack the carbonyl carbon of p-NPA. This assay is based on enzymatic hydrolysis from p-NPA to p-NP and acetate. Considering p-NP is a chromogenic compound that has a strong absorbance peak at 402 nm, as the progression of autohydrolysis, the absorbance of the reaction solution at 402 nm will gradually increase. Thus, the activity of the enzyme can be characterized by dividing it with the maximum absorbance of the same concentration of p-NP shown below. In this thesis, unless otherwise specified, the concentration of initial p-NPA is 0.25 mM and the catalyst concentration is 0.125 mM.

$$Conversion\ Rate\% = \frac{Solution\ Absorbance}{0.25\ mM\ p-NP\ Absorbance} * 100\%$$

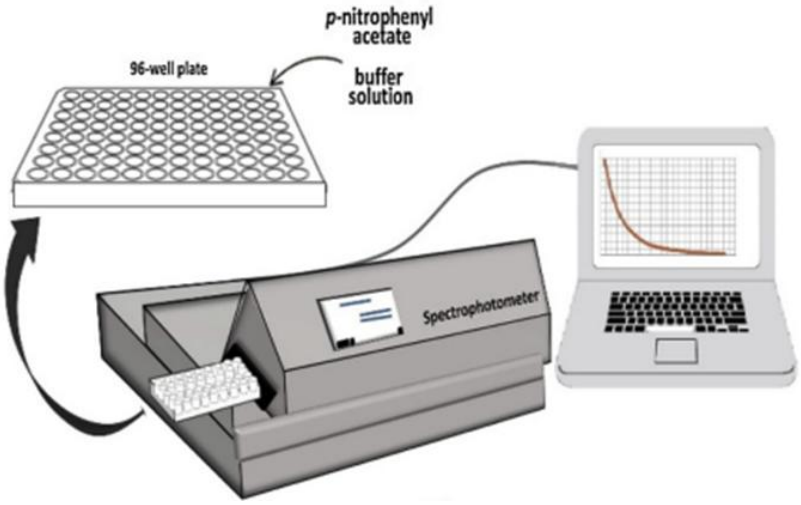

Fig 1.4 Apparatus for colorimetric characterization of carbonic anhydrase

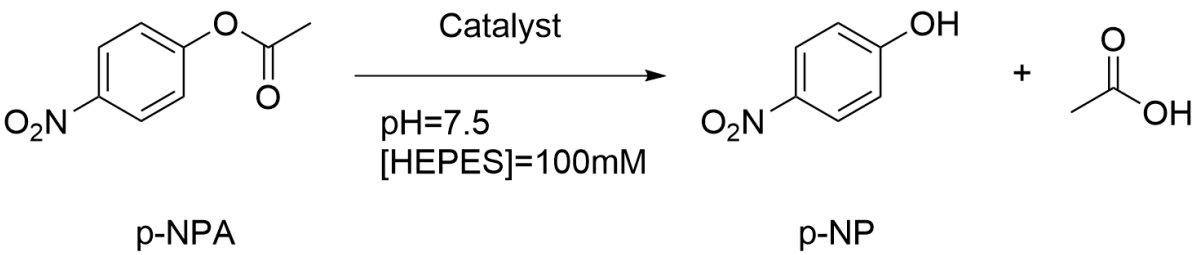

Fig 1.5 Illustration of catalyst involved hydrolysis reaction of p-NPA

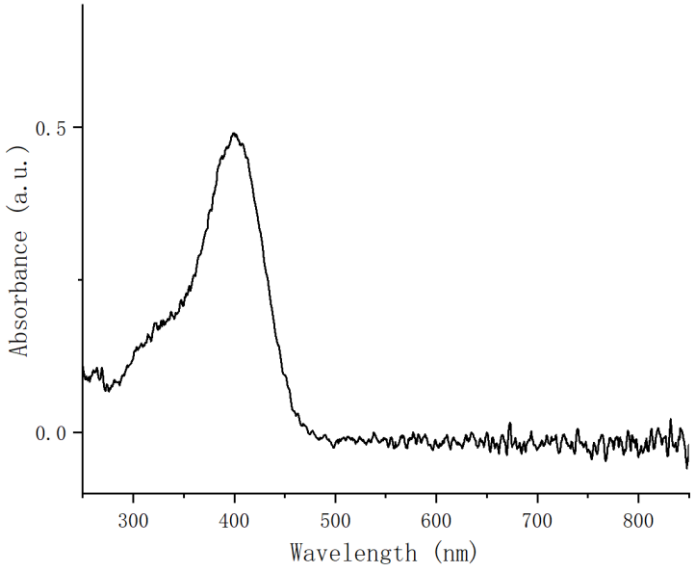

Fig 1.6 UV-vis spectrum of p-NP from 300nm to 500nm, strong absorbance peak observed at 402nm

II. Section 2. Experimental Methods

2.1 Materials and Synthesis

Synthesis of Nbrpe6Nce6Do3a, 1 equivalent of Nbrpe, 0.09 mmol, was synthesized in the auto synthesizer and then coupling reaction performed with bromoacetic acid following standard protocol. The resulting resin was washed with dimethylformamide (DMF) (3x) and DCM (3x). Displacement reaction was carried out by adding 0.45 mmol of 1,4,7,10-Tetraazacyclododecane-1,4,7,10-tetraacetic acid (Do3a), 0.18 mmol of K_2CO_3, 0.135 mmol tetrabutylammonium iodide (TBAI) and 3 ml of DMF into the cartridge to get. Reaction left shaking at room temperature for overnight. Resin washed with DMF (5x), DCM (3x0, and test cleavage carried out for 5h to confirm the formation of desired peptoid sequence.

Synthesis of Nbrpe6cyclen, Nbrpe6 resin (~10 mg, ~.007 mmol, 1 eq) was synthesized following standard synthesis protocol. The resin was then coupled with chloroacetic acid following standard coupling protocol (200 ul DIC/DMF, 1.5 ul 0.6 M chloroacetic acid (94.5 g/mol),). The resin was washed with DMF (3X). Then resin was transferred to a 20 mL round bottom flask, where 1,4,7,10-tetraazacyclododecane (Cyclen) (172.276 g/mol, 5 eq, .0287 mmol, .005 g) and triethyl amine (TEA) (101.19 g/mol, 1.2 eq, .0084 mmol, .00085 g) were dissolved into 300 ul of DMF. The reaction mixture then left at 50 °C for 45 minutes. The resin was then transferred into a cartridge and washed with DMF 3x and DCM 3X to yield Nbrpe6Cyclen.

Synthesis of Nbrpe6cyclenHis3, Nbrpe6cyclen coupled with chloroacetic acid (in excess, 3X

of standard amount) and left stirring for 1 h. The resulting resin washed with DMF (3X). Then excess amount of 2-(1H-imidazol-1-yl)ethanamine (Nhis) (3X of standard amount) in NMP into the cartridge for the displacement reaction and left at RT for 4 h. Finally, resin was washed with DMF and DCM 3X before test cleavage.

Synthesis of Nbrpm6cylenHis3, synthesis of this sequence carried out following the similar synthesis protocol as Nbrpe6cyclenHis3. Nbrpe6 was substituted to Nbrpm6.

Synthesis of Modified Nbrpe6Nme2NpmCyclenHis3, synthesis of this sequence carried out following the similar synthesis protocol as Nbrpe6cyclenHis3.

Nbrpe6cylenHis3-Zn^{2+} complex was also prepared for comparison use. To bind Zn^{2+} with peptoid, ~0.2 umol of peptoid powder was first dissolved with 95% TFA in a centrifuge tube. Then TFA was dried by gentle stream of Nitrogen gas flow until a viscous residue was visible on the bottom of the container. Pure acetonitrile and zinc salt acetonitrile solution added to dissolve TFA treated peptoid until the molar ratio between metal cation and peptoid monomers reached 1:1.

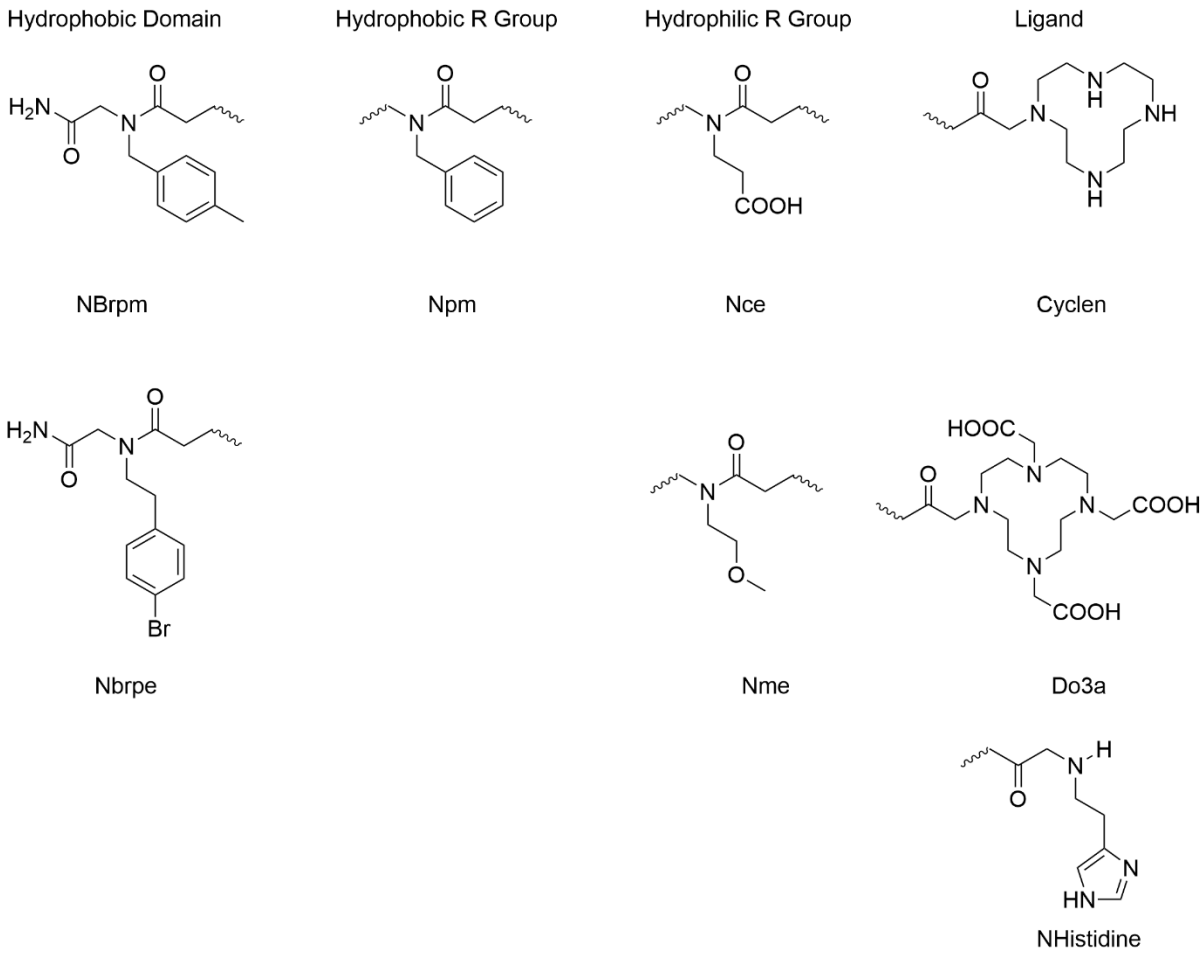

Fig 2.1 List of all the hydrophobic domain hydrophobic, hydrophilic side chains and ligands.

2.2 Peptoid Self-assembly & Recycling

Peptoid self-assembly was conducted by dissolving 1 μmol of corresponding peptoid into 200 μl acetonitrile/water mixture (1:1 by volume) to make a 5.0 mM clear solution. The solution is left under room temperature for slow evaporation to form gel-like solution. For co-assembly, a metal salt solution was added into the acetonitrile/water mixture and left for slow evaporation at 4 °C. Specifically, for Nbrpe6cyclenHis3, 0.5 M NaOH was added dropwise by using a P20 pipette to raise the pH of the mixture from 4.7 to the optimal self-assembly pH level between 5 to 7. The resulting solution was then allowed to equilibrate at room temperature and evaporate slowly for self-assembly.

For recycling peptoid-based catalysts, catalysts were recycled by centrifugation after each catalytic hydrolysis cycle. After hydrolysis, the reaction mixture solution was transferred into a centrifuge tube and centrifuged for 10 minutes at 14,000 rpm. Then the supernatant was removed by pipette and peptoid catalyst pellet was resuspended in deionized water for another round of centrifugation and removal of supernatant. After second round of wash, the pellet was resuspended with ~ 50μl of deionized water and lyophilized to power for further use.

2.3 Colorimetric Assay, Ultraviolet–visible spectrophotometry

The p-nitrophenyl acetate (p-NPA) assay is used to evaluate catalytic activity of each sequence. All hydrolysis reaction were performed in a Biotek Synergy LX plate reader. Each reaction mixture consisted of 255 μL of 100 mM HEPES buffer, 37.5 μL of 1 mM peptoid

solution, and 7.5 μL of 10 mM p-NPA dissolved in acetonitrile. The final concentration of catalyst and NPA was 0.125 mM and 0.25 mM respectively. Control samples were prepared by replacing the peptoid catalyst solution with an equal volume of deionized water. Each reaction mixture was deposited into separate wells of the microplate. To ensure reproducibility, 5 independent replicates of each sample were prepared and analyzed separately. UV–vis absorbance spectra were recorded from 300 nm to 500 nm with a stepwise of 2 nm at 15-minute intervals over 2 hours using a microplate reader under room temperature and in air.

2.4 Scan electron microscopy

Scanning electron microscopy (SEM) was carried out using a Thermo Scientific Apreo S system with OptiPlan mode. For SEM sample preparation, 2 μL of a 5 mM peptoid solution was diluted 50-fold with deionized water. 20 μL of the diluted solution was then deposited onto a clean silicon wafer substrate. Then the sample was incubated for 10 minutes at room temperature. Following incubation, excess solution was removed using filter paper. The sample was dried using a gentle stream of nitrogen gas and left overnight prior to imaging.

2.5 Atomic force microscopy

Atomic force microscopy (AFM) imaging was conducted using a Bruker ICON with ScanAsyst mode in air. Mica substrates were freshly cleaved immediately prior to sample deposition by applying and rapidly removing adhesive tape to expose a clean and flat surface. For sample preparation, 2 μL of a 5 mM peptoid stock solution was diluted 50-fold with

deionized water to reach the working concentration. The diluted solution was centrifuged at 14000 rpm for 5 mins. After centrifugation, the supernatant was removed, leaving only the pellet at the bottom of the centrifuge tube. 100ul of deionized water was added back in the tube. The pellet was resuspended in 100 µL of deionized water and subsequently sonicated for 10 minutes to further disperse any remaining aggregates. Following sonication, 20 µL of the resuspended solution was deposited onto the freshly cleaved mica surface and allowed to incubate for 15 minutes at room temperature. Excess liquid was gently removed using filter paper, and the substrate was dried with a stream of nitrogen gas prior to imaging.

2.6 Standard curve

To qualitatively analyze the conversion rate of p-NPA to p-NP, the maximum absorbance of the process was measured and plotted as a function of concentration. The conversion rate is calculated by subtracting the background absorbance and then divide by the maximum. P-NP exhibits a strong absorbance peak at 402 nm and the react solution gradually turns yellow. 50mM, 100mM, 150mM, 200mM and 250mM p-NP in HEPES buffer solution were prepared at 3 different pH levels. That is because HEPES buffer exhibited different extinction coefficient between neutral and basic environment and hydrolysis of p-NPA tends to react faster when pH level is higher. UV-Vis absorbances were measured 5 times at 402 nm with respect to each concentration and took the calculated average. The standard curve is shown below.

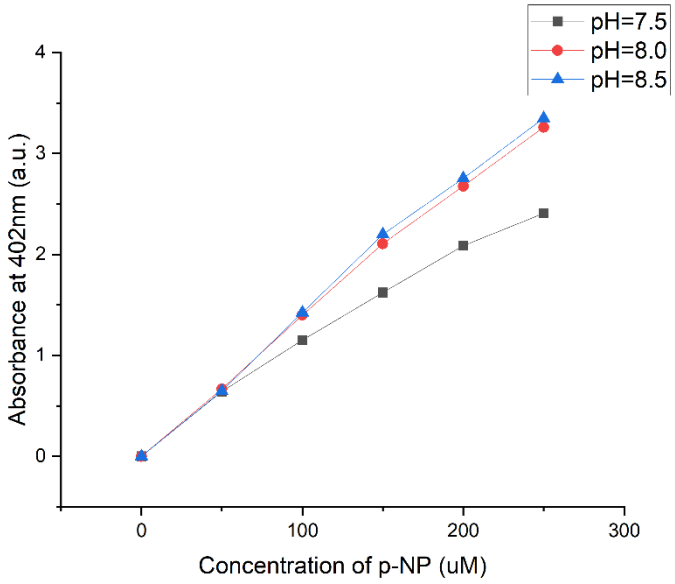

Fig 2.2 The maximum absorbance at 402 nm at different concentrations and pH levels of p-NP.

2.7 Stability Test

Stability tests were conducted to evaluate the structural stability of the self-assembled peptoid nanosheets under various conditions. 10 μL of 5 mM self-assembled peptoid solution was centrifuged at 14,000 rpm for 5 minutes. After removing the supernatant, an equal volume of deionized water was added to wash the pellet. The washed sample was characterized by AFM and labeled as "untreated" for reference. To assess stability, the peptoid was treated in various conditions. These included heating in deionized water at 60 °C and 90 °C for 2 hours, respectively, as well as heating in ethanol at 60 °C for 2 hours. In addition, the peptoid was incubated in pH 7.5 HEPES buffer overnight and again for 48 hours to examine its stability in buffered aqueous environments. Finally, the peptoid was recycled 5 consecutive times from the hydrolysis reaction mixture to evaluate its recyclability.

III. Section 3. Results and Discussion

3.1 Peptoid self-assembly

To generate peptoid with crystalline nanostructures, the corresponding peptoid powder was dissolved in water and acetonitrile (v/v=1:1) and left under room temperature for slow evaporation. Similarly, peptoids were co-assembled with Zn^{2+} ions by incubating them with an equimolar amount of $Zn(BF_4)_2$ solution (1:1 molar ratio). AFM results showed that peptoid sequences with 6 Nbrpe groups as its hydrophobic domain all formed nanosheets with high crystallinity. The height of the nanosheet is around 4 nm. The peptoid with 6 Nbrpm groups and cyclen formed irregular shaped flat nanostructure with a thickness of around 4 nm. According to the previous studies, sequences with Nbrpe and Nbrpm as their side chains

would form nanosheet and nanotube respectively[24,25]. Yet because of steric hindrance from bulky ligands adjacent to hydrophobic block, Nbrpm6cyclenHis3 is very hard to assemble to nanotube. The AFM and SEM images captured further confirmed that. Since peptoid's morphology of self-assembled nanostructures can be tuned. It is important to investigate the formed morphology's effect on the catalytic activity of the material. The catalytic activities of peptoid-based catalysts were determined by the colorimetric assay based on the hydrolysis of p-NPA at room temperature.

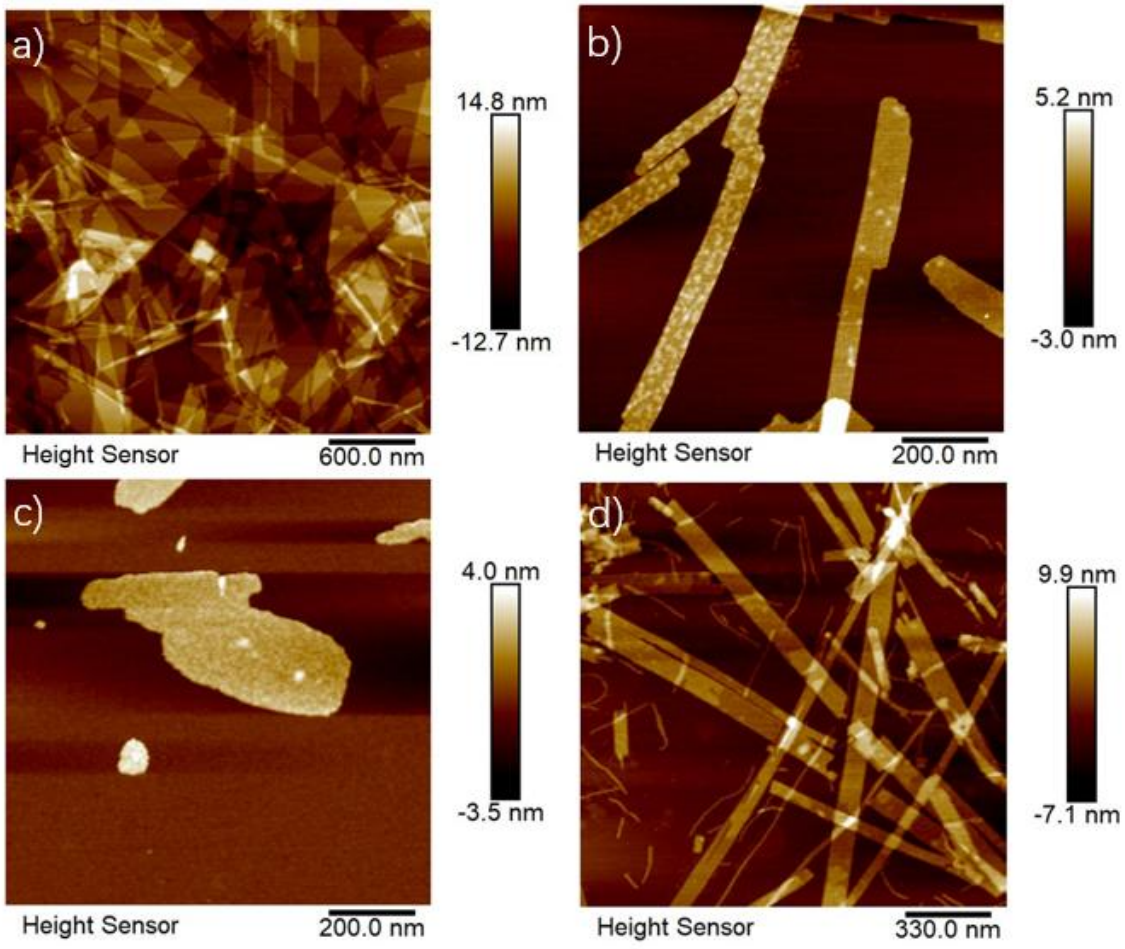

Fig 3.1 Representative AFM images for a) Nbrpe6Nce6 b) Nbrpe6cyclenHis3

c) Nbrpm6cyclenHis3 d) Nbrpe6Nme2NpmCyclenHis3

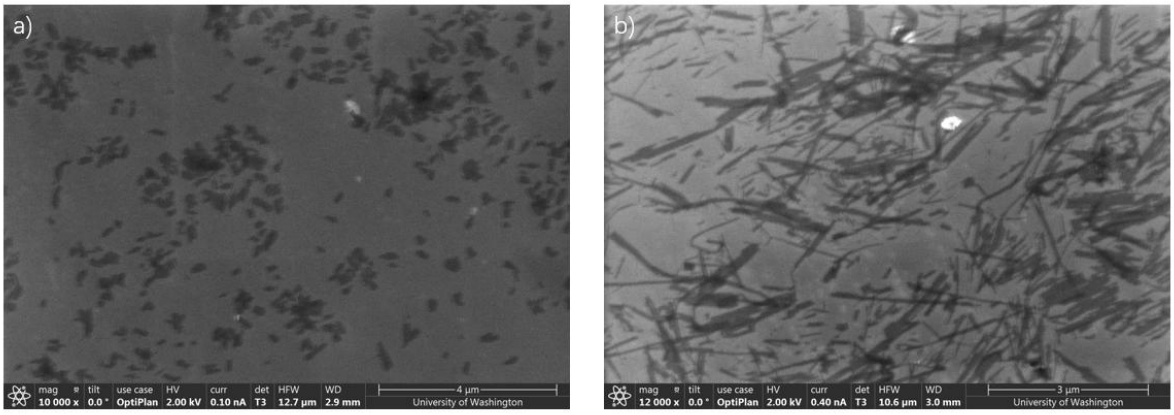

Fig 3.2 Representative SEM images of a) Nbrpm6cyclenHis3 b) Nbrpe6cyclenHis3

3.1 Activity Evaluation of Histidine Containing Sequences and Cofactor Free Sequences

The effect of morphology on catalytic activity was determined by tracing the Uv-Vis absorbance of p-NP at 402 nm. Then the conversion rate can be calculated. To mimic physiological pH, reaction was carried out in HEPES buffer at pH=7.5 and room temperature as the standard condition. Previous studies had suggested that assembled material's morphology could affect biomimetic catalyst's activity[22,26]. To further confirm its effect on histidine containing sequence, Nbrpe6cyclenHis3 monomer solution and its self-assembled solution were used to evaluate the degradation of p-NPA. According to the evolution curve and conversion rate curve, peptoid monomer solution showed almost identical changes of the absorbance compared to that of the control, which was the uncatalyzed CO_2 hydration reaction in neutral aqueous environment. While the self-assembled peptoid solution exhibited a significant and steady increase of absorbance at 402 nm during the 2-hour hydrolysis. The results verified that the peptoid-based catalyst's activity is brought by the interaction between self-assembled nanostructure and p-NPA. Peptoid monomer will not lower the activation energy of this reaction non-specifically.

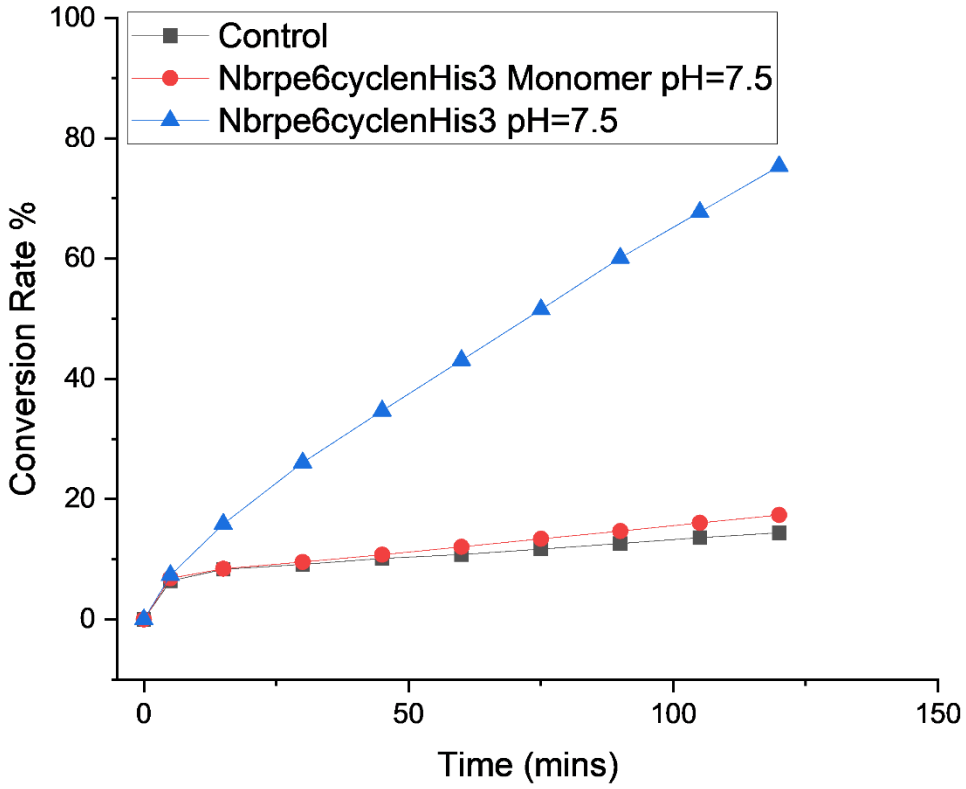

Fig 3.3 Conversion rates of control (DI water), self-assembled nanosheet and amorphous peptoid at standard condition

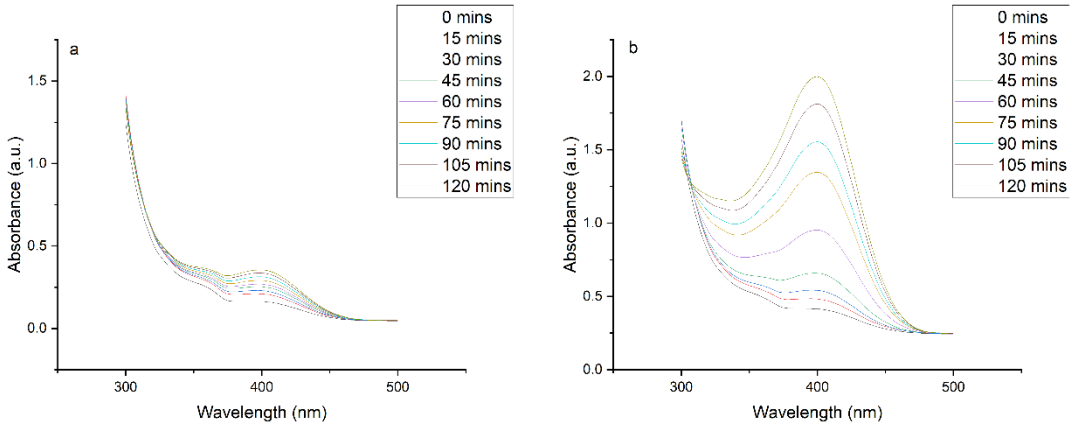

Fig 3.4 Absorbance evolution curve of a) amorphous peptoid b) self-assembled nanosheet

Since peptoid's morphology of nanostructure can be tuned by altering its hydrophobic domain[25]. To further investigate the effect of morphology on catalytic activity, Nbrpe6cyclenHis3 and Nbrpm6cyclenHis3 were evaluated and compared. Both sequences contain identical hydrophilic domains with three imidazole ligands but different hydrophobic domains. Both sequences exhibited high efficiency on catalyzing hydrolysis, still, Nbrpe6cyclenHis3 showed slightly higher activity than that of the Nbrpm6 containing sequence. It is hypothesized that this may be due to higher solvent accessible surface areas containing active sites with nanosheet than the amorphs structure.

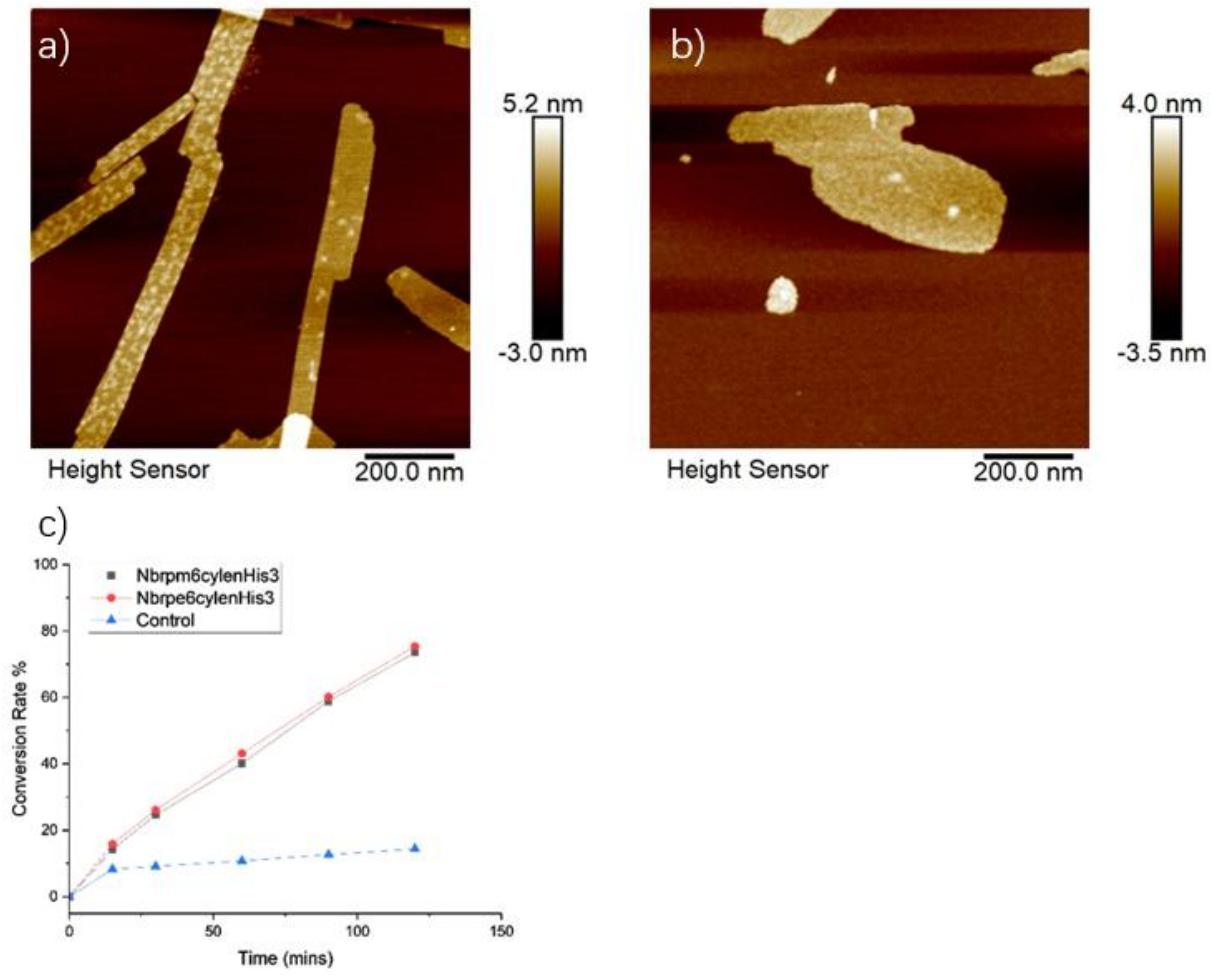

Fig 3.5 a) Representative AFM image of Nbrpe6cyclenHis b) Nbrpm6cyclenHis c) The conversion rates of both sequences under room temperature at pH=7.5

While natural CA shows high efficiency in catalyzing CO_2 hydration, its application is limited by the disadvantages in thermal and chemical stability[19,20,23]. Previous reports have shown that CA would denature and aggregate above 60 ℃ and in acidic environment[17]. Yet peptoid-based biomimetic catalysts have a significant advantage by exhibiting high stability. AFM results showed that Nbrpe6cyclenHis3 maintained its nanostructure in different conditions. Additionally, catalytic activity of recycled catalyst and freshly assembled catalyst were compared. A decrease of ~15% conversion rate in 2-hour hydrolysis has been observed. The decrease in catalytic activity may be due to the inevitable material loss during the process of centrifugation and recoveries. The solution of recycled peptoid was collected and centrifuged to collect the peptoid pellet. After lyophilization, among all 5 recycled peptoid pellet collected, ~5% of weight loss had been observed. It is also possible that during the process of recycling, centrifugation and sonication had mechanically degraded the formed nanostructures of peptoid. To further confirm this, the catalytic activities of 1-hour sonicated, 4-hour sonicated and untreated self-assembled Nbrpe6cyclenHis3 were evaluated and compared. However, no significant changes in catalytic activities were observed. Therefore, the main reason of loss of activity may still due to the loss of material.

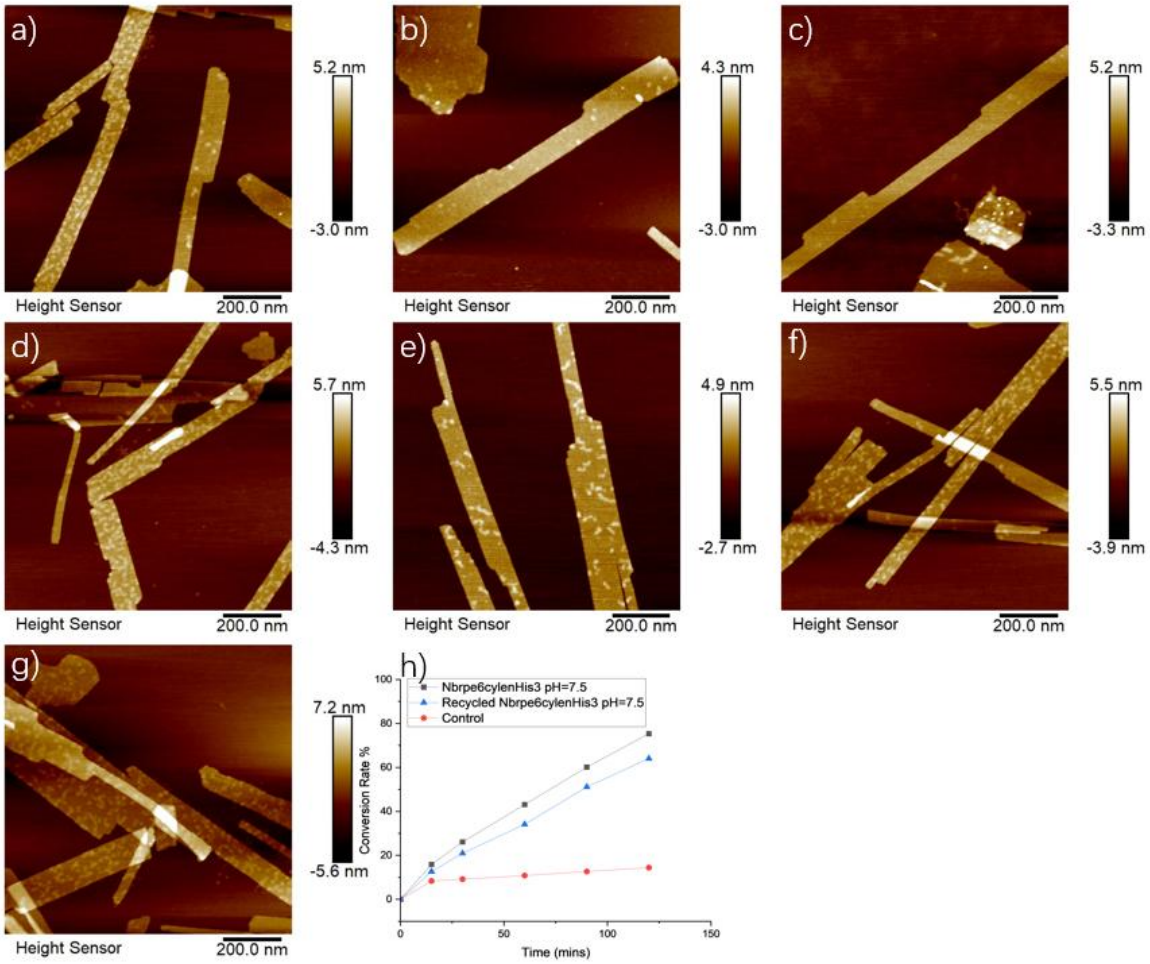

Fig 3.6 a) Self-assembled Nbrpe6cyclenHis3 b) Heated in deionized water for 2h at 60℃ c) Incubated in 100 mM HEPES buffer at pH=7.5 overnight d) Heated in deionized water for 2h at 90℃ e) Heated in ethanol for 2h at 60℃ f) incubated in 100 mM HEPES buffer at pH=7.5 for 48 hours g) Recycled Nbrpe6cyclenHis3 from completed hydrolysis reaction solution h) Conversion rates of recycled peptoid-catalyst and freshly assembled catalyst at pH=7.5

To investigate the ligand-metal coordination chemistry's effect on catalytic activity of biomimetic catalysts, Zn^{2+} bound Nbrpe6Nce6, Nbrpe6Nce6Do3a and Nbrpe6cyclen were evaluated and compared. Nbrpe6Nce6 and Nbrpe6Nce6Do3a exhibited relatively low conversion rate. The low activity of Nbrpe6Nce6 is due to the lack of efficient binding ligand for metal ion. There was no bounded ligand that allow metal ion to form the intermediate which is critical to the process of hydrolysis. However, it is interesting that Do3a containing sequence also exhibits low activity. Do3a ligand was designed with a structure of a cyclen group connecting with three carboxyl tails. The metal ion was supposed to interact with the ligand and function as the proton shuttle[27]. In this case, the efficiency of metal ion binding with the site was dramatically lowered. We hypothesized that the introduced substituents may increase steric hindrance around the active site and therefore potentially block the substrate. Also, carboxyl groups may compete for hydrogen bonding interactions and destabilizing the configuration. In contrast, Nbrpe6cyclen exhibits a higher activity. As mentioned above, CA's strong catalytic activity is attributed to the formation of tetrahedral Zn^{2+}-ligand coordination for optimized activity. Zn^{2+} acts as Lewis acid to produce hydroxyl anion from water, while at the same time, it directly takes part in the catalytic cycle via coordination and electrostatic effects. Later we also discovered low catalytic activity in Zn^{2+} bound Nbrpe6cyclenHis3 when comparing the activities of this sequence with and without the presence of cofactor. To confirm the reason for the decreased activity, a modification has been done to Nbrpe6cyclenHis3, 2 Nme and 1 Npm was added. The addition of Nmes can elongate the length of the hydrophobic domain that further decrease the steric hindrance with hydrophobic domain. The addition of Npm was for the substrate binding. From the results of

hydrolysis test, modified sequence showed lower catalytic activity to that of the Nbrpe6cyclenHis3 when there is no ion attached. Yet its activity increases after incubation with Zn^{2+}. The results fitted the expectation that such design could allow more space for metal-coordination.

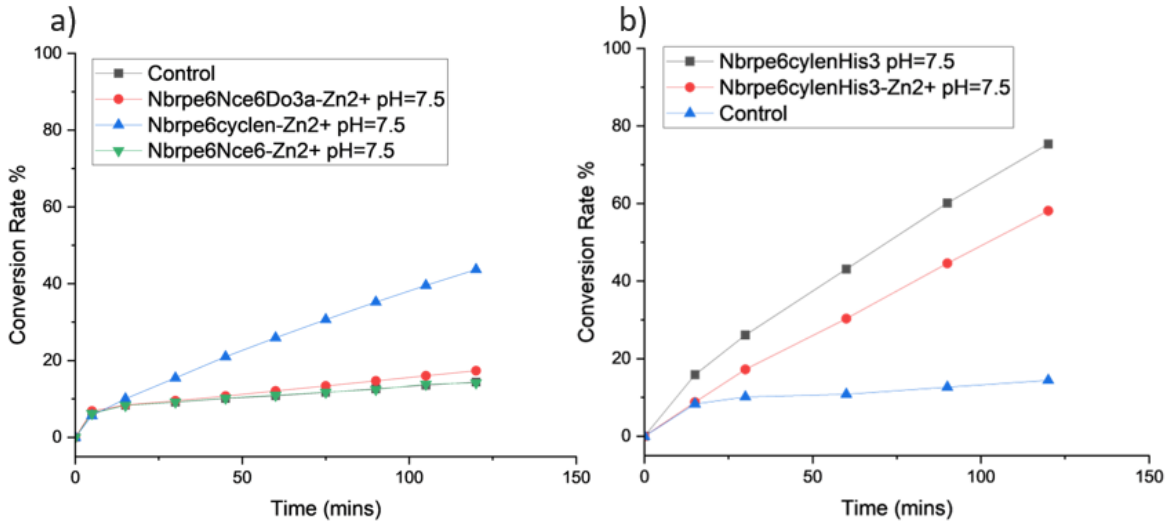

Fig 3.7 a) Conversion rates of a sequence without binding site (Nbrpe6Nce6), a sequence with the binding site (Nbrpe6cyclen) and a sequence with binding site and other ligands (Nbrpe6Nce6Do3a). b) Conversion rates of Nbrpe6cyclenHis3 before and after bind with Zn^{2+}

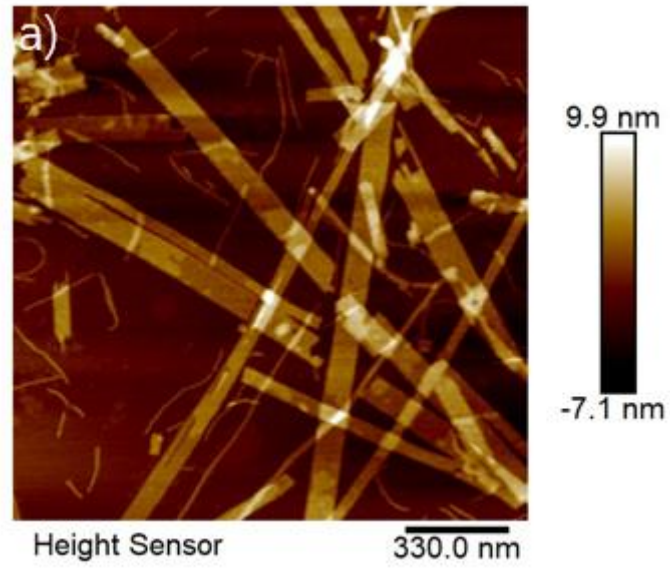

Fig 3.8 a) Representative AFM image of Nbrpe6Nme2NpmCyclenHis3

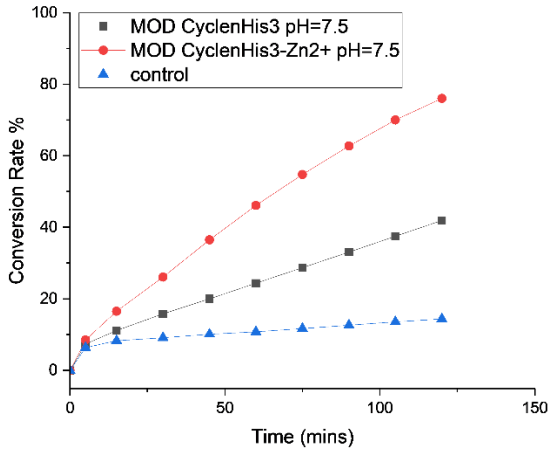

Fig 3.9 a) Conversion rates of Nbrpe6Nme2NpmCyclenHis3 before and after bind with Zn^{2+}

3.3 Catalytic Mechanism

Peptoid-based catalyst catalyzes ester hydrolysis through two plausible catalytic pathways. In the base catalyzed mechanism through extended hydrogen bonding network, imidazole functions as a general base, abstracting a proton from a nearby water molecule. The resulting hydroxide ion then acts as a nucleophile and attacks ester's carbonyl carbon, forming a

tetrahedral intermediate that collapses to release p-nitrophenol and acetate. Alternatively, a second mechanism suggests that the imidazole group itself may serve as a direct nucleophile, attacking the carbonyl carbon to form a transient covalent imidazole–acetyl intermediate. This intermediate is subsequently hydrolyzed by water, regenerating the free imidazole and completing the reaction.

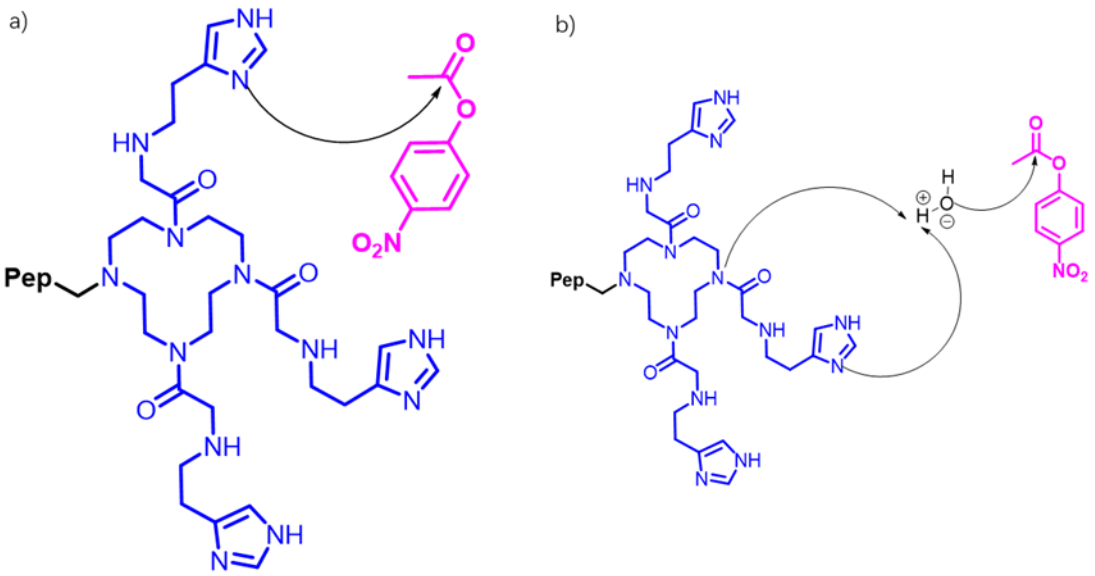

Fig 1.7 a) Direct hydrolysis pathway b) Base catalyzed pathway

Conclusion:

We explored the design and evaluation of peptoid-based biomimetic catalysts for enhancing the efficiency of carbon dioxide (CO_2) hydration, focusing on developing stable, efficient, and cofactor-free alternatives to natural carbonic anhydrase (CA). By taking advantage of the structural similarity between peptoids and peptides, a series of sequence-defined peptoids were synthesized to investigate the relationship between molecular design, morphology, and catalytic activity. The findings showed that self-assembled crystalline nanosheets, particularly those with high solvent-accessible surface areas, exhibited significantly higher catalytic efficiency than unassembled monomers or amorphous structures. The role of ligand-metal coordination was also examined by evaluating sequences assembled with and without Zn^{2+} binding. While Zn^{2+} coordination enhanced activity in some cases, steric hindrance introduced by certain ligands would diminish the performance. We synthesized and characterized a cofactor-free peptoid catalyst, Nbrpe6cyclenHis3, which exhibited robust catalytic activity and excellent thermal stability even in the absence of metal ions. This material maintained its structure under high temperature, extended incubation and retained high activity across multiple catalytic cycles. Our work further validates that peptoid-based materials are a promising platform for enzyme mimetics due to their programmability, chemical stability, and tunable assembly behavior.

Acknowledgement:

This work was supported by the US Department of Energy (DOE), Office of Science, Office of Basic Energy Sciences (BES) under an award FWP 80124 at Pacific Northwest National Laboratory (PNNL).

Part of AFM and SEM experiments were conducted at the Molecular Analysis Facility, a National Nanotechnology Coordinated Infrastructure (NNCI) site at the University of Washington, which is supported in part by funds from the National Science Foundation (awards NNCI-2025489, NNCI-1542101).

I would like to express my sincere gratitude to Dr. Chun-long Chen for his mentorship and invaluable guidance. I am deeply thankful to Dr. Progyateg Chakma, Dr. Thi Kim Hoang Trinh, Wenhao Zhou, Zeqian Zhang, Renyu Zheng, Qizheng Yang and Xuansheng Wang for their thoughtful suggestions and technical support. Thank Dr. Dan Graham, Scott Braswell and Yifeng Cai for their patience and the instrument training.

Reference

1) Sun, J.; Zuckermann, R. N. Peptoid polymers: a highly designable bioinspired material. *ACS Nano* **2013**, 7 (6), 4715-4732. DOI: 10.1021/nn4015714.

2) Xuan, S. Engineering the atomic structure of sequence-defined peptoid polymers and their assemblies *Polymer* **2020** Volume 202,122691

3) Lehn, J.-M. Toward Complex Matter: Supramolecular Chemistry and Self-Organization. *Proceedings of the National Academy of Sciences* **2002**, 99 (8), 4763–4768. doi.org/10.1073/pnas.072065599

4) Li, Z.; Cai, B.; Yang, W.; Chen, C.-L. Hierarchical Nanomaterials Assembled from Peptoids and Other Sequence-Defined Synthetic Polymers. *Chem. Rev.* **2021**, 121 (22), 14031–14087. doi.org/10.1021/acs.chemrev.1c00024.

5) Guler, M. A self-assembled nanofiber catalyst for ester hydrolysis. *J. Am. Chem.* Soc**. 2007**, 129, 40, 12082–12083

6) Liu, Q.; Kuzuya, A.; Wang, Z-G. Supramolecular enzyme-mimicking catalysts self-assembled from peptides **2023,** *iScience* Volume 26, Issue 1, 105831 doi.org/10.1016/j.isci.2022.105831

7) Kim, T.; Jian, T.; Jin, B.; Nguyen, D.-T.; Zuckermann, R. N.; Chen, C.-L. Designed Metal-Containing Peptoid Membranes as Enzyme Mimetics for Catalytic Organophosphate Degradation. *ACS Applied Materials & Interfaces* **2023**, 15 (44), 51191–51203. doi.org/10.1021/acsami.3c11816.

8) Olivier, G, K.; Cho, A.; Sanii. B.; Connolly, M, D.; Tran, H.; Zuckermann, R, N. Antibody-Mimetic Peptoid Nanosheets for Molecular Recognition. *ACS Nano* **2013**, 7,

10, 9276–9286 doi.org/10.1021/nn403899y

9) Cai, B.; Li, Z.; Chen, C.-L. Programming Amphiphilic Peptoid Oligomers for Hierarchical Assembly and Inorganic Crystallization. *Acc. Chem. Res.* **2021**, *54* (1), 81-91. DOI: 10.1021/acs.accounts.0c00533.

10) Jian, T., Zhou, Y., Wang, P. *et al.* Highly stable and tunable peptoid/hemin enzymatic mimetics with natural peroxidase-like activities. *Nat Commun* **2022,** 13, 3025. doi.org/10.1038/s41467-022-30285-9

11) Fan, F.; Zheng, Y.; Zhang, Y.; Zheng, H.; Zhong, J.; Cao, Z. A Comprehensive Understanding of Enzymatic Degradation of the G-Type Nerve Agent by Phosphotriesterase: Revised Role of Water Molecules and Rate-Limiting Product Release. *ACS Catal.* **2019**, *9* (8), 7038– 7051, doi.org: 10.1021/acscatal.9b01877

12) Effendi, S.; S. W.; Ng, I-Son. The Prospective and Potential of Carbonic Anhydrase for Carbon Dioxide Sequestration: A Critical Review. *Process Biochemistry* **2019**, 87, 55–65. doi.org/10.1016/j.procbio.2019.08.018.

13) Chen, C. L.; Beatty, A. M. Guest inclusion and structural dynamics in 2-D hydrogen-bonded metal-organic frameworks. *J. Am. Chem. Soc.* **2008**, *130* (51), 17222-17223. DOI: 10.1021/ja806180z.

14) Mandal, D.; Nasrolahi Shirazi, A.; Parang, K. Self-assembly of peptides to nanostructures. Org. Biomol. Chem. 2014, 12 (22), 3544-3561, 10.1039/C4OB00447G. DOI: 10.1039/C4OB00447G.

15) Brooks, S. C.; Jin, R.; Zerbach, V. C.; Zhang, Y.; Walsh, T. R.; Rosi, N. L. Single Amino Acid Modifications for Controlling the Helicity of Peptide-Based Chiral Gold

Nanoparticle Superstructures. J. Am. Chem. Soc. 2023, 145 (11), 6546-6553. DOI: 10.1021/jacs.3c00827

16) Lindskog, S. Structure and Mechanism of Carbonic Anhydrase. *Pharmacology & Therapeutics* **1997**, 74 (1), 1–20. doi.org/10.1016/s0163-7258(96)00198-2

17) Supuran, C. T. Structure and Function of Carbonic Anhydrases. *The Biochemical Journal* **2016**, 473 (14), 2023–2032. doi.org/10.1042/BCJ20160115.

18) Silverman, D. The catalytic mechanism of carbonic anhydrase: implications of rate-limiting protolysis of water. *Acc. Chem. Res*. **1988**, 21, 1, 30–36 doi.org/10.1021/ar00145a005

19) Zimmerman, S. Inhibition of archaeal and bacterial carbonic anhydrases. *Bioorganic & Medicinal Chemistry*, **2007**, 15(22), 7058–7066. doi.org/10.1016/j.bmcl.2007.05.045

20) Cimmperman, P. Protein thermal denaturation measurements via fluorescent dye. *RSC Biomolecular Sciences.* **2011**, 408(2), 277–279

21) Liu, Q. Cofactor-free oxidase-mimetic nanomaterials from self-assembled histidine-rich peptides. *Nature. Materials* **20**, 395–402 (2021). doi.org/10.1038/s41563-020-00856-6

22) Li, Z. Supramolecular peptide nanostructures regulate catalytic efficiency and selectivity *Angew.Chem. Int. Ed.* **2023**, 62, e202303755. doi.org/10.1002/anie.20230375

23) Kim, J.H.; Jo, B.H. A Colorimetric CO_2 Hydration Assay for Facile, Accurate, and Precise Determination of Carbonic Anhydrase Activity. *Catalysts* **2022**, *12*, 1391. doi.org/10.3390/catal12111391

24) Ma, J.; Cai, B.; Zhang, S.; Jian, T.; De Yoreo, J. J.; Chen, C.-L.; Baneyx, F. Nanoparticle Mediated Assembly of Peptoid Nanosheets Functionalized with Solid-Binding Proteins:

Designing Heterostructures for Hierarchy. Nano Lett. 2021, 21 (4), 1636–1642. doi.org/10.1021/acs.nanolett.0c04285.

25) Shao, L.; Hu, D.; Zheng, S-L,; Trinh, T.; Zhou, W.; Wang, H.; Zong, Y.; Li, C.; Chen, C-L. Hierarchical Self-Assembly of Multidimensional Functional Materials from Sequence-Defined Peptoids *Angew.Chem Int.* **2024** Volume63, Issue24 doi.org/10.1002/anie.202403263

26) Rufo, C. Short peptides self-assemble to produce catalytic amyloids. *Nature. Chemistry* **2014**, 303-309 (2014) doi.org/10.1038/nchem.1894

Gamba, I. Biomimetic approach to CO_2 reduction *Bioinorganic Chemistry and Applications/Volume* **2018**, Issue 1/2378141